

XAFS analysis of high-energy implanted Ni atoms into Si(100)

Shiro ENTANI^{1,*}, Shin-ichiro SATO¹, Mitsunori HONDA² and Takeshi OHSHIMA¹¹ Takasaki Advanced Radiation Research Institute,

National Institutes for Quantum Science and Technology,

1233 Watanukimachi, Takasaki, Gunma 370-1292, Japan

² Materials Science Research Center, Japan Atomic Energy Agency,

2-4 Shirakata, Tokai, Ibaraki 319-1195, Japan

1 Introduction

Ni silicide synthesis by Ni ion beam irradiation into Si attracts attention due to its advantages including the ability of formation of local structures, the controllability of ion beams, the formability of silicide without heat treatment and the high reproducibility of the resulting specimen. It has been reported that the buried NiSi₂ layer was synthesized by 6 MeV Ni irradiation located at around 3.0 μm from the surface [1], although the formation mechanism has not been clarified. The atomic structure of deeply implanted Ni into Si should be characterized to elucidate the formation mechanism of NiSi₂ by Ni ion implantation. Ni *K*-edge fluorescence yield X-ray absorption fine structure (XAFS) is a powerful technique for this kind of characterization, because the X-ray absorption length (1/*e* attenuation) in Si at the energy of Ni *K*-edge (8333 eV) is calculated to be more than 10 μm [2] so that the atomic and electronic structure of deeply buried Ni atoms can be analyzed properly. In this work, we investigate the evolution of the NiSi₂ synthesis during 3.0 MeV Ni⁺ ions irradiation ranging from 10¹³ to 10¹⁶ ions·cm⁻². The local atomic structure of Ni implanted in Si is clarified by analyzing Ni *K*-edge fluorescent XAFS.

2 Experiment

Heavily doped p-type Si(100) substrates with a 300 nm thermally oxidized SiO₂ layer were ultrasonically cleaned by acetone, methanol and ultra-pure water. The Si(100) specimens were irradiated with 3.0 MeV Ni⁺ ions at room temperature. The irradiation experiments were carried out at Takasaki Ion accelerator for Advanced Radiation Application (TIARA), National Institutes for Quantum Science and Technology (QST). The Ni ion fluence was varied from 10¹³ to 10¹⁶ ions·cm⁻². The atomic structure and the electronic states of Ni⁺-irradiated Si specimens were analyzed by XAFS. The Ni *K*-edge XAFS spectra were collected in the fluorescence mode at BL-27B hard X-ray beamline at the Photon Factory of High Energy Research Organization (KEK-PF).

3 Results and Discussion

Figure 1 (a) shows Ni *K*-edge EXAFS spectra of Ni⁺-irradiated Si. Differences arose in the fine structure of the spectra between the ion fluences below 10¹⁴ ions·cm⁻² and above 10¹⁵ ions·cm⁻². These features are clearly seen in the *k*²-weighted $\chi(k)$ spectra of Ni *K*-edge EXAFS shown in Fig. 1 (b). The Fourier transforms (FTs) of the EXAFS

spectra with a *k*-range of below 8.5 Å⁻¹ are shown in Fig. 1 (c). In the FTs with the ion fluences lower than 10¹⁴ ions·cm⁻², two prominent structures are observed at around 1.7 and 2.2 Å, which are attributed to the Ni-Si bond in NiSi₂ and the Ni-Ni bond in metallic face-centered cubic (fcc) Ni, respectively [3,4]. It can be considered that the high diffusivity of Ni in crystalline Si [5] causes segregation and clustering of implanted Ni atoms as well as the formation of NiSi₂. The peak from the Ni-Ni bond disappears after the Ni irradiation at the fluence above 10¹⁵ ions·cm⁻². It can be said that the formation of NiSi₂ promotes significantly with the ion fluence above 10¹⁵ ions·cm⁻², although it is currently uncertain whether the Ni-Ni bond changed to the Ni-Si bond or the small Ni-Ni signal buried in the large Ni-Si signal.

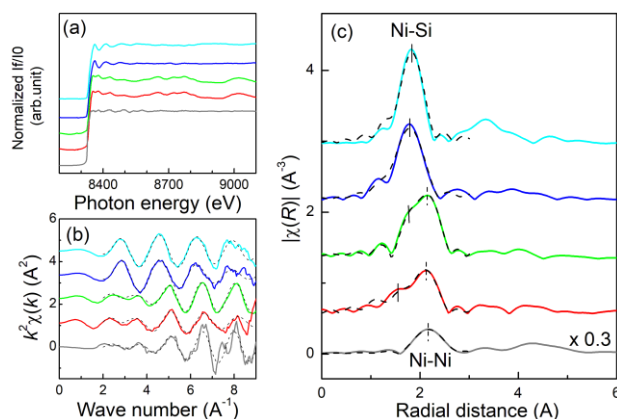


Fig. 1: (a) EXAFS spectra, (b) *k*²-weighted $\chi(k)$ spectra and (c) Fourier transformations (FTs) of the EXAFS spectra. Grey, red, green, blue and sky blue lines in (a,b,c) are spectra of Ni foil, 10¹³, 10¹⁴, 10¹⁵, 10¹⁶ ions·cm⁻²-irradiated Si, respectively. The simulated fitting curves (dotted line) are also indicated.

Here we discuss the atomic structure such as bond pair and intrinsic distance of Ni implanted in Si through EXAFS analysis. Table 1 summarized the Ni-Si and Ni-Ni bond length in the Ni-implanted Si. These values are the average of calculated results obtained from three difference places on the same specimen. In the case of the 10¹³ and 10¹⁴ ions·cm⁻², the FTs can be fitted with two single-scattering paths (Ni-Si in NiSi₂ and Ni-Ni in fcc Ni). The difference of the Ni-Si bond length in Ni-irradiated Si from the bulk crystal is larger for the 10¹⁴ ions·cm⁻² irradiation than that for the 10¹³ ions·cm⁻² irradiation. This

is though to be originated from the increase in lattice strains due to the accumulation of radiation induced damage and implanted Ni atoms. In contrast, the FTs can be fitted with a Ni-Si single-scattering path in the case of 10^{15} and 10^{16} ions·cm⁻². These results indicate that at the fluence above 10^{15} ions·cm⁻² the NiSi₂ phase is dominantly formed and the Ni-Ni bond formation is less dominant.

Table 1: Ni-Si and Ni-Ni bond lengths of Ni atoms implanted in Si. These values are the average of calculated results obtained from three different places on the same specimen.

Fluence (ions·cm ⁻²)	Ni-Si length (Å)	Ni-Ni length (Å)
10^{13}	2.27 ± 0.03	2.45 ± 0.02
10^{14}	2.65 ± 0.02	2.50 ± 0.01
10^{15}	2.33 ± 0.02	–
10^{16}	2.31 ± 0.01	–
	2.36 (NiSi ₂ on Si(111)) [6]	2.48 ± 0.02 (Ni foil)

It is found from the results described above that the increase in the concentration of Ni did not lead to the increase in the formation of the Ni-Ni bond. The implanted Ni atoms prefer to form the NiSi₂ phase with the Ni-Si bond and this fact can be explained by the structural modification of Si lattice due to ion irradiation. Ion beams lose their energy in the material and causes displacements of the lattice atoms via the nuclear energy depositions. As the ion fluence increases to a critical value, the accumulated damage produces a continuous amorphous region in the crystal. According to the Kinchin-Pease model, the displacements per atom is calculated by considering kinetic energy transfers above a threshold of the displacement energy; $T_d/2E_d$, where T_d is the damage energy (the nuclear energy deposition) and E_d is the displacement energy of lattice atoms [7]. Thus, the critical fluence D_c for Si-amorphization is expressed as $D_c = 2E_d N_{Si} / T_d$, where N_{Si} is density of silicon atoms. With using $E_d = 15$ eV, $T_d = 2.1 \times 10^9$ eV·cm⁻¹ [8] and $N_{Si} = 5.0 \times 10^{22}$ atoms·cm⁻³, D_c is calculated to be 7.1×10^{14} ions·cm⁻².

This value can be experimentally substantiated by Raman spectroscopy. Figure 2 shows Raman spectra of Ni-irradiated Si with different fluence. The most intense peak at 520.7 cm⁻¹ and the peak at 303 cm⁻¹ are attributed to transverse optics (TO) and the second-order transverse acoustic (2TA) mode of Si lattice, and both peaks decrease with increasing ion fluence. For the Ni-irradiated Si with the fluence of 10^{15} and 10^{16} ions·cm⁻², the peak from TO mode broadened significantly and shifted lower wavenumbers. This indicates the amorphization appears at the fluence above 10^{15} ions·cm⁻² [9].

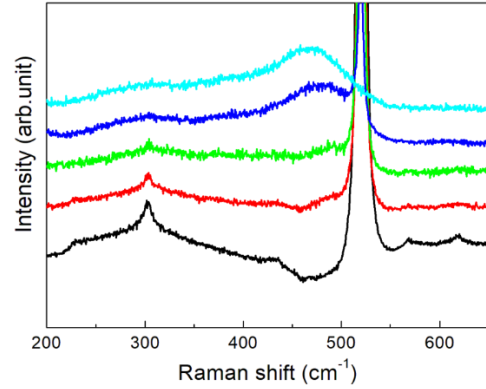


Fig. 2: Raman spectra of pristine Si (black), Ni⁺-irradiated Si at the fluence of 10^{13} ions·cm⁻² (red), 10^{14} ions·cm⁻² (green), 10^{15} ions·cm⁻² (blue) and 10^{16} ions·cm⁻² (sky blue).

In conclusion, we have studied the local atomic structure of deeply buried Ni atoms in Si by high-energy ion irradiation. We found that the significant difference arose in bond pair and intrinsic distance of Ni atoms according to the difference in the ion fluence. The Ni *K*-edge fluorescent-yield EXAFS analysis showed that Ni atoms have mixed structure of metallic-like fcc Ni and NiSi₂ phase at the initial state of the Ni irradiation and that the formation of NiSi₂ promotes significantly with the ion fluence above 10^{15} ions·cm⁻². With consideration of the critical fluence for Si-amorphization ($D_c = 7.1 \times 10^{14}$ ions·cm⁻²), the amorphization of Si due to the accumulation of irradiation induced damage is key to obtain the NiSi₂ phase in Ni⁺-irradiated Si.

References

- [1] J.K.N. Lindner *et al.*, *Nucl. Instrum. Methods Phys. Res. Sect. B Beam Interact. Mater. At.* **59-60**, 655 (1991).
- [2] W.H. McMaster *et al.*, *COMPILATION OF X-RAY CROSS SECTION.*, California Univ., Livermore. Lawrence Radiation Lab., United States, 1969.
- [3] S.J. Naftel *et al.*, *Phys. Rev. B* **57**, 9179 (1998).
- [4] A. Fernandez *et al.*, *Mater. Trans.* **44**, 2055 (2003).
- [5] N. Yarykin *et al.*, *Appl. Phys. Lett.* **109**, 102101 (2016).
- [6] D. Cherns *et al.*, *Philos. Mag. A.* **46**, 849 (1982).
- [7] G.H. Kinchin and R.S. Pease, *Rep. Prog. Phys.* **18**, 1 (1955).
- [8] J.P. Biersack and J.F. Ziegler, SRIM-2013.00, <http://www.srim.org/>.
- [9] D.M. Zhigunov *et al.*, *Appl. Phys. Lett.* **113**, 023101 (2018).

* entani.shiro@qst.go.jp